Ergosterol promotes pheromone signaling and plasma membrane fusion in mating yeast

Hui Jin,[1] J. Michael McCaffery,[2] and Eric Grote[1]

[1]Department of Biochemistry and Molecular Biology, Johns Hopkins Bloomberg School of Public Health, Baltimore, MD 21205
[2]Integrated Imaging Center, Johns Hopkins University, Baltimore, MD 21218

Ergosterol depletion independently inhibits two aspects of yeast mating: pheromone signaling and plasma membrane fusion. In signaling, ergosterol participates in the recruitment of Ste5 to a polarized site on the plasma membrane. Ergosterol is thought to form microdomains within the membrane by interacting with the long acyl chains of sphingolipids. We find that although sphingolipid-free ergosterol is concentrated at sites of cell–cell contact, transmission of the pheromone signal at contact sites depends on a balanced ratio of ergosterol to sphingolipids. If a mating pair forms between ergosterol-depleted cells despite the attenuated pheromone response, the subsequent process of membrane fusion is retarded. Prm1 also participates in membrane fusion. However, ergosterol and Prm1 have independent functions and only *prm1* mutant mating pairs are susceptible to contact-dependent lysis. In contrast to signaling, plasma membrane fusion is relatively insensitive to sphingolipid depletion. Thus, the sphingolipid-free pool of ergosterol promotes plasma membrane fusion.

Introduction

The fusion of two or more cells to form a larger hybrid is a fundamental process required for sexual reproduction and the development of multinuclear cells including muscle fibers, placental trophoblasts, and osteoclasts (Chen and Olson, 2005). Emerging results indicate that cell fusion also contributes to the progression of malignant diseases and to tissue regeneration by stem cells (Duelli and Lazebnik, 2003; Ogle et al., 2005). The defining event of cell fusion is the merger of two plasma membranes. Although the mechanisms of membrane fusion during intracellular transport and viral infection have been intensively investigated, there is a relative paucity of information about how membranes fuse from their extracellular surfaces in the absence of viral fusion proteins. The *Caenorhabditis elegans* protein Eff-1 is currently the most promising candidate fusogen. Eff-1 is essential for fusion of epithelial cells during development (Mohler et al., 2002), and ectopic expression of Eff-1 in naive cells promotes cell fusion (Podbilewicz et al., 2006). However, Eff-1 homologues have not been identified in other species. Mating in the yeast *Saccharomyces cerevisiae* provides an amenable genetic system that may reveal features common to diverse types of cell fusion.

Correspondence to Eric Grote: egrote@jhsph.edu

Abbreviations used in this paper: FLZ, fluconazole; FRET, fluorescence resonance energy transfer; $PI(4,5)P_2$, phosphatidylinositol-4-phosphate; PO, propylene oxide; SC, synthetic complete; YPD, yeast peptone dextrose.

The online version of this paper contains supplemental material.

Yeast mating begins with an exchange of pheromone signals between haploid cells of the opposite mating type (Elion, 2000; Bardwell, 2005). The mating pheromones bind to specific receptors that transmit their signals via a common heterotrimeric G protein. G protein activation leads to polarized recruitment of signaling proteins to the cell surface. These proteins include Cdc42, Far1, Bni1, Ste20, and the components of a MAPK cascade comprising the scaffold protein Ste5 and the kinases Ste11, Ste7, and Fus3. Among the targets of the Fus3 MAPK are Far1, which arrests the cell cycle in G1, and Ste12, the transcription factor that activates expression of mating-associated genes. After a 30-min delay, cells of the opposite mating type bind to each other to form mating pairs, which are also referred to as prezygotes. A carefully orchestrated program of cell wall remodeling then begins. The cell walls of the mating pair are first joined into a unified structure, and then the cell walls at the junction between the two cells are selectively degraded (Gammie et al., 1998). Once the intervening cell walls have been removed, the plasma membranes of the two apposing cells come into contact and fuse to form a zygote. Mating is subsequently completed by fusion of the two nuclei followed by budding of a diploid daughter cell.

In cell fusion mutants, mating pairs form but fail to fuse, leading to an accumulation of prezygotes (White and Rose, 2001). Accumulation of early prezygotes with intact cell walls separating the two partner cells indicates a cell wall remodeling defect, whereas accumulation of late prezygotes with plasma membranes

The Journal of Cell Biology, Vol. 180, No. 4, February 25, 2008 813–826
http://www.jcb.org/cgi/doi/10.1083/jcb.200705076

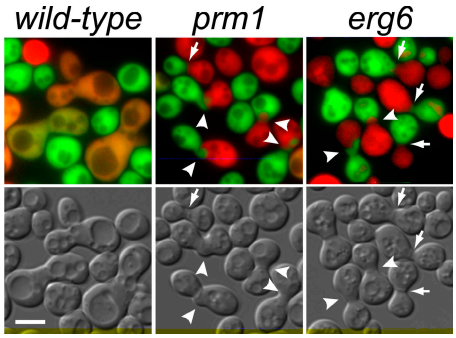

Figure 1. **Late prezygotes in the *erg6* mutant.** *MATa* cells expressing cytoplasmic GFP were mated to *MATα* cells expressing cytoplasmic RFP. Fused zygotes (yellow) are found in the wild type. Late prezygotes (arrowheads) in the *erg6* and *prm1* mutants have a finger of green or red cytoplasm projecting from one cell into its mating partner. Early prezygotes (arrows) have a flat interface between cells. Bar, 5 µm.

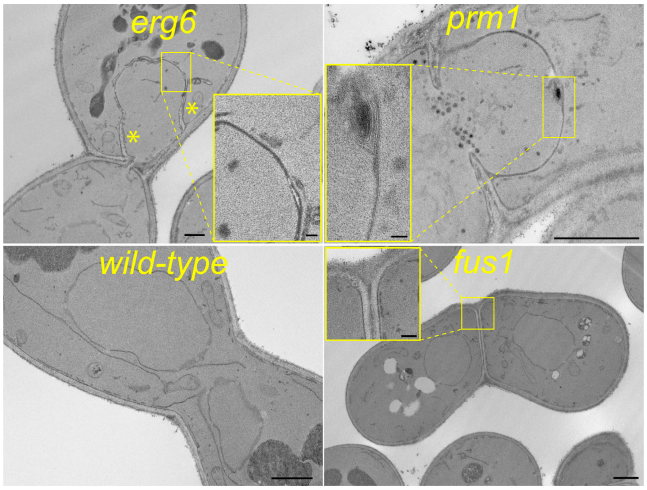

Figure 2. **Plasma membrane apposition in an *erg6* mating pair.** Cytoplasmic fingers delineated by two directly opposed plasma membranes are found in the *erg6* and *prm1* mating pairs. Cell walls growing at the base of the *erg6* cytoplasmic finger are marked with asterisks. The *prm1* mating pair has a myelin-like whorl (inset). The wild-type mating pair has completed fusion. The *fus1* mating pair has cell walls separating the two plasma membranes. Insets show magnifications of the areas in the yellow rectangles. Bars: 2 µm (images); 0.1 µm (insets).

in contact indicates defective membrane fusion. Although many genes are known to be involved in cell wall remodeling, the pheromone-regulated membrane protein Prm1 was the first and, until recently, the only protein implicated in plasma membrane fusion (Heiman and Walter, 2000). In addition to accumulating late prezygotes, the two cells in a *prm1* mutant mating pair are prone to simultaneous lysis once their plasma membranes come into contact, suggesting that Prm1 stabilizes the assembly of nascent fusion pores (Jin et al., 2004; Aguilar et al., 2006). Once a fusion pore forms, it must expand to permit the nuclei to fuse. Fusion pore expansion is regulated by Fus1, which also has a critical but independent role in cell wall remodeling (Nolan et al., 2006).

Although phospholipid bilayer membranes are typically viewed as passive participants in protein-mediated membrane fusion, the lipid composition of a membrane has profound effects on biophysical properties that may affect a membrane's fusability, including intrinsic curvature, thickness, stiffness, and permeability. Compared with intracellular membranes, the yeast plasma membrane is highly enriched in ergosterol, just as mammalian plasma membranes are highly enriched in cholesterol (Schneiter et al., 1999). Within a membrane, sterols can interact with the long saturated acyl chains of sphingolipids to dynamically partition into membrane microdomains, which are often referred to as lipid rafts (Mukherjee and Maxfield, 2004; Hancock, 2006). Rafts are thought to form by dense packing of the flexible acyl chains of sphingolipids against the flat rigid sterol molecule to produce a thickened liquid-ordered phase membrane, which still permits rapid lateral diffusion. Association of proteins with a membrane fraction that is resistant to detergent extraction at 4°C is commonly cited as evidence that the proteins are concentrated in lipid rafts, but it is now understood that chilling cells and extracting phospholipids can induce interactions that do not exist in living cells (Lichtenberg et al., 2005). Furthermore, the large (micrometer scale) and stable liquid-ordered microdomains found in artificial membranes at reduced temperatures do not exist in most biological membranes. Instead, lipid raft–associated glycosylphosphatidylinositol-anchored proteins have an apparently uniform cell surface distribution by confocal microscopy, and sophisticated fluorescence resonance energy transfer (FRET) techniques were required to detect <5-nm clusters of three to four proteins (Sharma et al., 2004). Indeed, the difficulty of unambiguously detecting nanometer-scale domains in living cells has led some to question whether lipid rafts actually exist (Munro, 2003; Douglass and Vale, 2005). One emerging model is that functional membrane microdomains are formed via cooperative interactions between nanoscale lipid domains, membrane-associated proteins, and the actin cytoskeleton (Viola and Gupta, 2007).

We uncovered two ergosterol biosynthesis genes in a visual screen for yeast mutants arrested at the plasma membrane fusion stage of mating. Plasma membrane ergosterol promotes rapid fusion and acts independently of the Prm1 protein. Ergosterol depletion also interfered with the response to mating pheromones, but robust pheromone signaling was not essential for membrane fusion. Sphingolipids were depleted to investigate the potential involvement of lipid rafts in signaling and fusion. Signaling depends on a balanced ratio of ergosterol to sphingolipids, whereas fusion is more dependent on the total amount of ergosterol, indicating that signaling and fusion are regulated by different pools of ergosterol.

Results

Discovery of the *erg6* mating defect

The yeast knockout collection was screened for mutants that were defective at the plasma membrane fusion stage of mating by crossing pairs of *MATa* and *MATα* strains with the same gene deleted in each mating partner (Fig. S1, available at http://www.jcb.org/cgi/content/full/jcb.200705076/DC1). Most cell fusion mutants accumulate only early prezygotes, but late prezygotes that were identical to those originally described for *prm1* were

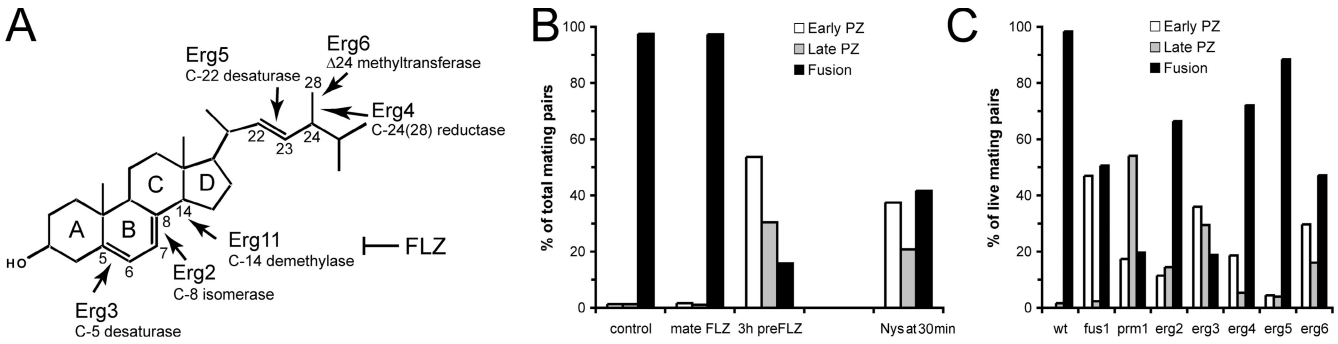

Figure 3. **Ergosterol biosynthesis and plasma membrane fusion.** (A) Enzymes and inhibitors of the ergosterol biosynthesis pathway. (B) FLZ and nystatin (Nys) inhibit plasma membrane fusion. Wild-type cells were mated for a total of 100 min on SC plates supplemented with 1 mg/ml FLZ or 32 µg/ml Nys. For the 3-h pre-FLZ sample, *MATa* and *MATα* cultures were separately incubated with FLZ for 3 h in liquid culture before mating on FLZ plates. The Nys at 30 min was transferred from an SC plate to an SC + Nys plate at 30 min of mating. The Nys at 30 min data is from a different experiment than the other three data sets. (C) *erg* mutant matings. wt, wild type.

readily detected in an *erg6* mating, implicating ergosterol in plasma membrane fusion (Fig. 1).

Electron microscopy confirmed that the two plasma membranes of an *erg6* mating pair could be in intimate contact over an extended zone of apposition (Fig. 2). For comparison, many *prm1* mating pairs also had an extended zone of membrane apposition, whereas the two plasma membranes in *fus1* mating pairs were separated by cell walls. Two additional features are documented in the *prm1* mating pair: clustered vesicles adjacent to the cell wall remnants and a myelin sheath-like whorl formed from the two plasma membranes at one point within the zone of plasma membrane apposition. Similar features were described in an earlier study of yeast mating (Gammie et al., 1998) and were also found in some *erg6* mating pairs. Finally, the *erg6* and *prm1* mating pairs both have cell wall fragments near the base of the cytoplasmic finger that lie perpendicular to the remnant cell wall separating the two plasma membranes. Thus, the cell wall may be able to regenerate at a later time if plasma membrane fusion is inhibited.

Phenotypic differences between *erg6* and *prm1*

Similar to *prm1*, the *erg6* mating phenotype is heterogeneous, containing a mixture of fused mating pairs and early and late prezygotes (Fig. 3). However, *erg6* matings had a higher proportion of early prezygotes as well as an increased percentage of haploid cells that did not engage a mating partner, suggesting that ergosterol is also involved in an earlier step in the mating pathway (see Fig. 5). A further distinction between *erg6* and *prm1* is that the percentage of *erg6* mating pairs with cytoplasmic projections declined over time with an accompanying increase in fused mating pairs (unpublished data). Thus, plasma membrane fusion is delayed rather than blocked by altering the sterol composition of cellular membranes.

The dynamics of individual cell fusion events were examined by time-lapse imaging of *MATa erg6 GFP* cells mating to *MATα erg6 RFP* cells. Similar to previous results with *prm1* (Nolan et al., 2006), fusion pore permeance calculated from the rate of GFP diffusion between cells was not strongly reduced in *erg6* mating pairs (unpublished data). Under standard time-lapse imaging conditions, the two cells of a *prm1* mating pair often lyse after achieving plasma membrane contact (Jin et al., 2004; Nolan et al., 2006). The lysis/fusion ratio was >50 in *prm1* mating pairs but <0.1 in wild-type mating. In the *erg6* videos, there were 29 fusions and 5 simultaneous lysis events. Thus, we conclude that the two plasma membranes of an *erg6* mating pair are susceptible to lysis once they come into contact, but they are substantially more stable during fusion than *prm1* membranes. The differences between the *erg6* and *prm1* phenotypes suggest that ergosterol and Prm1 might function in different processes leading to plasma membrane fusion.

Plasma membrane ergosterol promotes fusion

To confirm the importance of ergosterol during plasma membrane fusion, wild-type mating pairs were treated with antibiotics that inhibit ergosterol biosynthesis or bind to plasma membrane ergosterol. Fluconazole (FLZ) is an azole antibiotic that interferes with lanosterol demethylation, an essential step in the ergosterol biosynthetic pathway (Fig. 3 A). Treatment with 1 mg/ml FLZ, a dose which is 200-fold above the ID_{50}, has no effect on the growth rate of a log-phase culture for the first 6 h, indicating that the preexisting pool of ergosterol is sufficient for essential functions until it is turned over and/or diluted by expansion of the culture (Fig. S2 A, available at http://www.jcb.org/cgi/content/full/jcb.200705076/DC1). Nevertheless, ergosterol synthesis is immediately inhibited, leading to lanosterol accumulation within 30 min (Fig. S2 B). Prezygotes were not detected when yeast were mated on FLZ plates, indicating that ongoing ergosterol synthesis is not essential for mating. However, late prezygotes accumulated when *MATa* and *MATα* cells were individually pretreated with FLZ for 3 h before mating (Fig. 3 B). The cellular ergosterol concentration that promotes plasma membrane fusion must be higher than that required for growth because a 3-h FLZ pretreatment inhibits fusion but has no effect on the growth rate.

Nystatin is a polyene antibiotic that binds to ergosterol in the yeast plasma membrane and eventually forms channels in the membrane leading to cell lysis (Silva et al., 2006). Yeast treated with 32 µg/ml nystatin failed to form mating pairs, but late

prezygotes were found when mating pairs were allowed to assemble during a 30-min preincubation and then transferred to a nystatin plate. Importantly, the two cells of these late prezygotes maintained their cytoplasmic fluorescence, which is an indication that they had not yet lysed. The FLZ and nystatin mating results indicate that the plasma membrane pool of ergosterol contributes to cell fusion and argue against the alternative possibility that newly synthesized ergosterol in the secretory pathway is needed to target a fusion protein to sites of plasma membrane contact.

Structural features of ergosterol that modulate membrane fusion

Although zymosterol synthesis is essential for aerobic growth, later steps in the ergosterol synthesis pathway are not, and the late enzymes do not obligatorily act in a linear pathway (Parks and Casey, 1995; Heese-Peck et al., 2002). To identify structural features of ergosterol that are important for cell fusion, *MATa GFP* and *MATα RFP* strains with deletions in each of the nonessential *erg* genes were mated and scored for prezygote accumulation. Mutations in *erg2*, *3*, and *6* inhibited plasma membrane fusion, whereas mutations in *erg4* and *5* did not (Fig. 3 C). Thus, plasma membrane fusion appears to depend on both a proper double bond configuration in the B ring (*erg2* and *3*) and methylation of the tail (*erg6*), although it is possible that one or more of the *erg* mutations inhibits fusion indirectly by altering the activity of other enzymes in the ergosterol biosynthesis pathway. Some of the *erg* mutants have actin polarity, endocytosis, and/or homotypic vacuole fusion phenotypes (Kato and Wickner, 2001; Heese-Peck et al., 2002), but the subset of *erg* mutants with mating defects is unique. In particular, *erg3*, which had the strongest plasma membrane fusion defect, does not interfere with α-factor binding, localization and endocytosis of the α-factor receptor, or the polarized distribution of actin patches and cables (Heese-Peck et al., 2002). We conclude that the mating phenotype is unlikely to be an indirect consequence of defects in these other processes.

Interactions between *PRM1* and ergosterol

The *prm1* and *erg* mutations have low penetrance, allowing a significant level of plasma membrane fusion even when they are deleted from both cells in a mating pair. Fusion was normal in *erg6* cross wild-type matings, regardless of whether the mutation was in the *MATa* or *MATα* cell, as was previously shown for *prm1* and many other cell fusion mutants (Heiman, and Walter, 2000). In contrast, there was essentially no plasma membrane fusion and an increased accumulation of late prezygotes when two *prm1 erg6* double-mutant strains were mated (Fig. 4 A). Similar results were obtained with double-mutant combinations between *prm1* and *erg2* or *3*. The additive effect of the *prm1* and *erg* mutations supports the conclusion that Prm1 and ergosterol function in independent processes leading to plasma membrane fusion.

One implication of the double-mutant results is that ergosterol depletion does not inhibit mating by interfering with Prm1 targeting to sites of cell–cell interaction. This inference was directly tested by depleting ergosterol with a FLZ pretreatment and then observing the localization of GFP-Prm1 in arrested

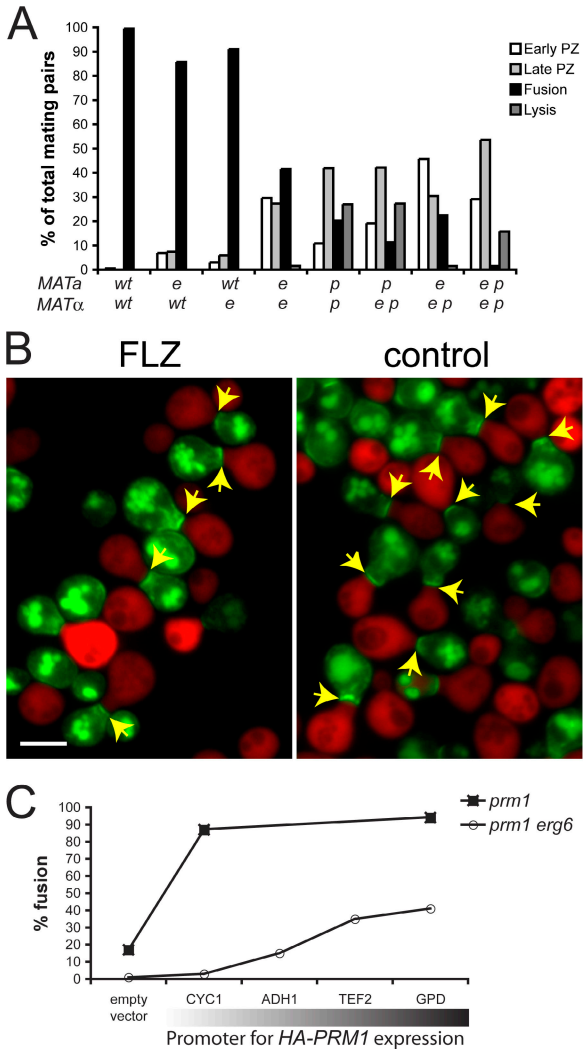

Figure 4. **Interactions between *PRM1* and ergosterol.** (A) Matings between combinations of wild-type (wt), *erg6* (e), *prm1* (p), and *erg6 prm1* double-mutant (ep) strains. (B) GFP-Prm1 localization in arrested mating pairs. *MATa GFP-PRM1* cells were mated to *MATα fus1 fus2 RFP* cells to accumulate early prezygotes. The arrows mark GFP-Prm1 (green) localized to sites of cell–cell contact in early prezygotes. Ergosterol was depleted with a 3-h FLZ pretreatment. Bar, 5 μm. (C) Enhanced reliance on Prm1 expression for plasma membrane fusion in *erg6* mating pairs. Plasmids directing *HA-PRM1* expression from various promoters were transformed into pairs of *MATa* and *MATα* strains.

mating pairs (Fig. 4 B). GFP-Prm1 was concentrated at sites of cell–cell contact in 71.4% of the FLZ-pretreated early prezygotes (n = 388) compared with 74.9% of the untreated controls (n = 339).

To examine the effect of varying Prm1 expression on plasma membrane fusion, an HA epitope-tagged form of the *PRM1* gene was placed under the control of a series of constitutively active promoters (Mumberg et al., 1995). Western blotting with an anti-HA antibody confirmed that the *GPD* promoter yielded the highest HA-Prm1 expression, with progressively lower expression from the *TEF*, *ADH1*, and *CYC* promoters (unpublished data). When these plasmids were transformed into both mating partners, HA-Prm1 expression from the weak *CYC1* promoter was sufficient to restore normal mating to *prm1* mutant mating pairs.

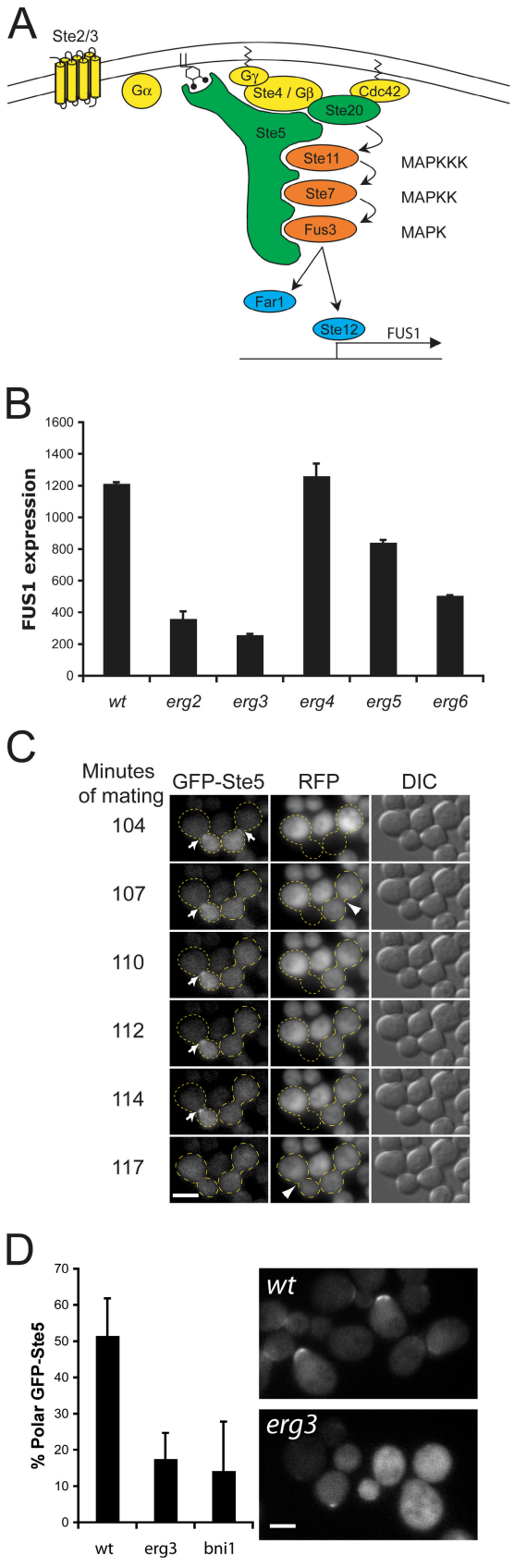

Figure 5. **Ergosterol promotes Ste5 recruitment during pheromone signaling.** (A) Illustration of the pheromone signaling pathway. (B) Ergosterol biosynthesis mutations alter the transcriptional response to mating pheromones. FUS1 expression is shown in arbitrary units. Error bars represent the standard deviation. (C) Dynamics of GFP-Ste5 localization in yeast mating pairs. *MATa GFP-STE5* cells were mated to *MATα RFP* cells. RFP transfer (arrowheads) indicates plasma membrane fusion. GFP-Ste5 is concentrated at the site of cell–cell contact (arrows) before fusion and is then rapidly redistributed throughout the cytoplasm of the zygote. (D) Ergosterol promotes GFP-Ste5 recruitment to the tips of mating projections. Error bars represent 95% confidence intervals. wt, wild type. Bars, 5 μm.

In contrast, a progressive increase in Prm1 expression yielded a progressive increase in cell fusion in *prm1 erg6* double-mutant mating pairs (Fig. 4 C). Thus, ergosterol depletion enhances the dependence of plasma membrane fusion on high Prm1 expression. Interestingly, only the highest level of *PRM1* expression driven by the *GPD* promoter was sufficient to restore mating to the efficiency found when *PRM1* is expressed from its native promoter in the *erg6* mutant.

Ergosterol promotes pheromone signaling

erg6 matings had a high percentage of haploid cells that failed to interact with a mating partner. The *erg6* mutant also had a diminished morphogenic response to pheromones, with a lower percentage of cells extending mating projections to form the pear-shaped cells known as shmoos. These observations suggested that sterols modify the response to mating pheromones. To further investigate this possibility, quantitative measurements of the transcriptional response to mating pheromones in *erg* mutant strains were made with a P_{FUS1}-*lacZ* reporter construct (Fig. 5 B). The results showed a positive correlation between reduced *FUS1* induction and defective plasma membrane fusion, with *erg3* showing the strongest defect in both processes.

Because ergosterol is concentrated in the plasma membrane (Schneiter et al., 1999), we tested the hypothesis that ergosterol depletion inhibits membrane-localized events in the pheromone signaling pathway. One critical signaling event is recruitment of the Ste5 MAPK scaffold to polarized sites on the plasma membrane. As illustrated in Fig. 5 A, Ste5 binds to Gβγ and Cdc24 (a nucleotide exchange factor for Cdc42) and interacts with membrane lipids via an N-terminal amphipathic helix known as the plasma membrane domain and a cryptic pleckstrin homology domain, both of which are specific for phosphatidylinositol-4-phosphate (PI(4,5)P_2; Whiteway et al., 1995; Pryciak and Huntress, 1998; Winters et al., 2005; Garrenton et al., 2006). As a MAPK scaffold, Ste5 recruits the Ste11, Ste7, and Fus3 kinases to the membrane. The ultimate effect of recruiting Ste5 to the membrane is to facilitate phosphorylation of Ste11 by Ste20, thereby activating the MAPK cascade.

Ste5 recruitment was examined using a GFP-Ste5 fusion protein. In wild-type *MATa* cells, α-factor triggers rapid translocation of a portion of the intracellular pool of GFP-Ste5 to a focused spot on the plasma membrane that corresponds to the future site of mating projection growth (Pryciak and Huntress, 1998; Mahanty et al., 1999). In mating pairs, GFP-Ste5 was found at sites of cell–cell contact until the moment of fusion, when it diffused throughout the cytoplasm of the fused zygote (Fig. 5 C). The percentage of nonbudded cells with a polarized GFP-Ste5 spot was reduced in the *erg3* mutant (Fig. 5 D), suggesting that ergosterol promotes recruitment of a signaling complex to the

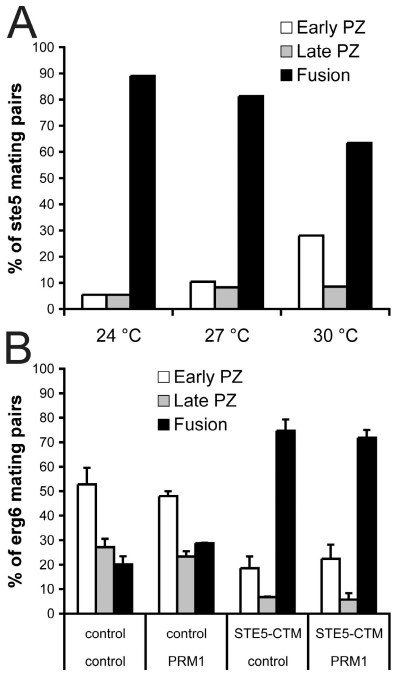

Figure 6. **Influences of pheromone signal intensity on plasma membrane fusion.** (A) Reduced pheromone signaling does not cause late prezygote accumulation. Pairs of *ste5^{ts}* strains were mated for 100 min at the indicated temperatures. (B) Amplification of the pheromone response enhances fusion in *erg6* mating pairs. Error bars represent the standard deviation.

plasma membrane. The *bni1Δ* mutant was used as a control for this experiment because the actin cable nucleation activity of Bni1 was previously shown to facilitate GFP-Ste5 translocation (Qi and Elion, 2005). In contrast to *bni1*, the *erg3* mutant has normal actin cables (Heese-Peck et al., 2002), indicating that the failure to recruit GFP-Ste5 is not caused by an underlying defect in cell polarization. In conclusion, altering the sterol composition of the plasma membrane interferes with recruitment of Ste5 to the site of signaling.

The critical role of Ste5 recruitment was further defined by an epistasis experiment with Ste5-CTM, a chimeric protein in which the transmembrane anchor of Snc2 is fused to the C terminus of Ste5 (Pryciak and Huntress, 1998). Targeting of Ste5-CTM to the plasma membrane restored pheromone signaling to ergosterol-depleted cells (Fig. S3, available at http://www.jcb.org/cgi/content/full/jcb.200705076/DC1), confirming that ergosterol depletion inhibits membrane-localized events in the pheromone signaling pathway.

The relationship between pheromone signaling and plasma membrane fusion

An identical subset of ergosterol biosynthesis mutants reduced both pheromone signaling and plasma membrane fusion (Figs. 3 C and 5 B). Given the central role of pheromones in regulating the overall mating process, a reduction in pheromone responsiveness might indirectly cause the plasma membrane fusion defect. To investigate this possibility, cell fusion was assayed in the temperature-sensitive *ste5^{ts}* mutant, which fails to mate at 34°C (Hartwell, 1980). Adjusting the temperature of *ste5^{ts}* cells acts as a rheostat to control the degree of pheromone-induced *FUS1* expression without creating a subpopulation of nonresponsive cells (Fig. S4, available at http://www.jcb.org/cgi/content/full/jcb.200705076/DC1). Thus, this mutant provides an ideal system for examining the effect of reduced pheromone responsiveness. In a 24°C mating reaction, <10% of *ste5^{ts}* mating pairs arrested before fusion (Fig. 6 A). Early prezygotes accumulated at 30°C, potentially because of reduced expression of *FUS1* and other pheromone-regulated genes that are involved in cell wall remodeling, but there was not a significant accumulation of late prezygotes. Apparently, a higher level of signaling is required for the completion of cell wall remodeling than for plasma membrane fusion. A similar defect in cell wall remodeling, but not plasma membrane fusion, was previously found in mutants with reduced a-factor synthesis (Brizzio et al., 1996). The more modest pheromone signaling defect of a *bni1* mutation (Qi and Elion, 2005) did not result in accumulation of either early or late prezygotes in our standard mating conditions. Because a robust pheromone response is not essential for plasma membrane fusion, reduced pheromone signaling cannot be the sole cause of the membrane fusion defect associated with ergosterol depletion.

Because the pheromone-regulated protein Prm1 had to be expressed at high levels to promote fusion in *erg6* mating pairs, we examined the effect of boosting the pheromone response to above normal levels (Fig. 6 B). *erg6* cells induced with a combination of α-factor and *STE5-CTM* had twofold higher P_{FUS1}-*lacZ* expression than wild-type cells induced with α-factor alone. In a mating reaction, *STE5-CTM* expression reduced the number of *erg6* cells that could form mating pairs by 70% (unpublished data), possibly by binding to Gβγ and thereby competitively inhibiting Gβγ–Far1 interactions (Butty et al., 1998; Winters et al., 2005). However, the mating pairs that were able to form between *STE5-CTM*–expressing *erg6* cells were more likely to fuse and less likely to arrest as either early or late prezygotes. Only a small fraction of this increased fusion was recapitulated by *PRM1* overproduction, indicating that additional pheromone-regulated processes contribute to the efficiency of both cell wall remodeling and plasma membrane fusion. These processes could include posttranslational activation and polarized recruitment of fusion proteins and/or synthesis of additional pheromone-regulated genes. *STE5-CTM* expression also promoted fusion of wild-type cells that were mated in suboptimal conditions (synthetic complete [SC] galactose plates for 3 h at 30°C), raising the percentage of fused pairs from 92 to 98%. In conclusion, the membrane fusion defect resulting from ergosterol depletion can be overcome by enhancing the efficiency of other processes leading to fusion.

Polarized targeting of free ergosterol in mating pairs

It was previously proposed that lipid rafts enriched in ergosterol and sphingolipids contribute to mating by facilitating the targeting of Fus1 and other membrane proteins to mating projections (Bagnat and Simons, 2002). The proposal that lipid rafts contribute to membrane protein targeting has been challenged by others (Valdez-Taubas and Pelham, 2003), and we found no obvious defect in Fus1-GFP targeting to mating projections in the *erg* mutants (unpublished data). If lipid rafts were required for Fus1 targeting, ergosterol depletion should inhibit the

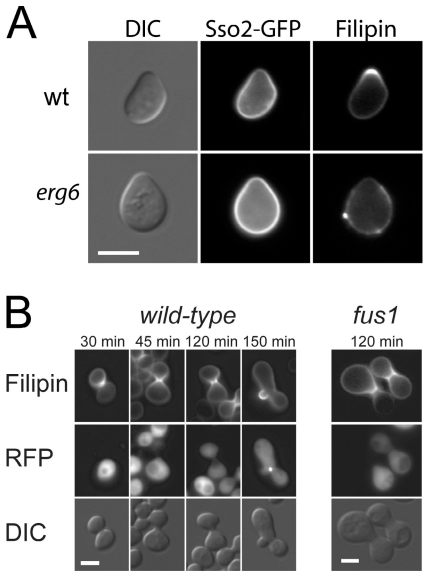

Figure 7. **Ergosterol polarity in yeast mating.** (A) *MATa SSO2-GFP* cells were treated with α-factor and then stained with filipin. wt, wild type. (B) Filipin stains sites of cell–cell contact before and after fusion. Wild-type and *fus1* mutant cells were mated for the indicated times and then stained with filipin. Bars, 5 μm.

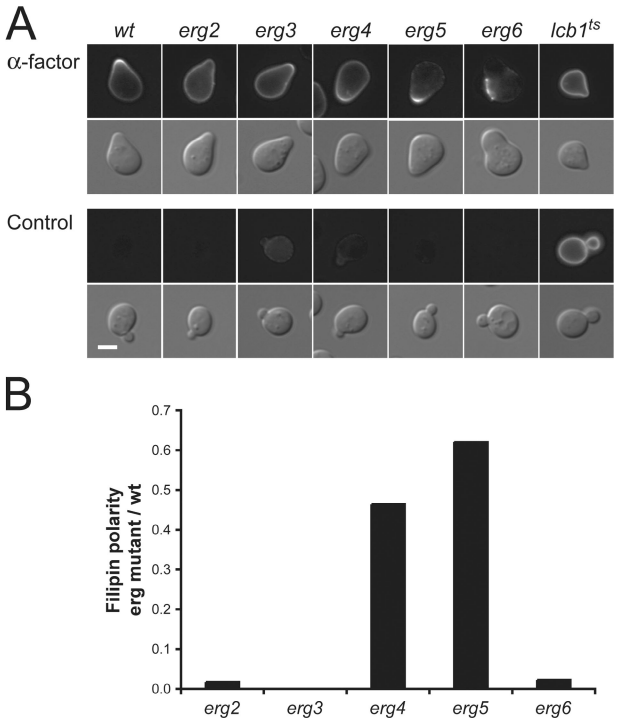

Figure 8. **Filipin staining of lipid biosynthesis mutants.** (A) Cells of the indicated strains were treated with our without α-factor and then stained with filipin. Bar, 5 μm. (B) Quantification of filipin polarization in α-factor–treated cells.

Fus1-dependent processes of cell wall remodeling and fusion pore expansion. In contrast, ergosterol depletion inhibits pheromone signaling and plasma membrane fusion, as shown in Figs. 1–3 and 5. We therefore conclude that the plasma membrane fusion defect in *erg* mutant mating pairs is not caused by a primary defect in lipid raft–mediated membrane protein targeting.

An important observation, which was originally used to support the concept that lipid rafts promote polarized transport, is that filipin, a sterol ligand, stains the tip of the mating projection in shmoos (Bagnat and Simons, 2002). We confirmed this observation using a more rapid filipin staining procedure (see Materials and methods) to preferentially stain the plasma membrane and minimize the time available for sterol redistribution (Fig. 7 A). The bright filipin staining at the shmoo tip does not represent a general increase in the density of plasma membrane because the plasma membrane protein Sso2-GFP is not concentrated there. In genuine mating pairs, filipin stained sites of cell–cell contact (Fig. 7 B). Polarized filipin staining was maintained in arrested *fus1* prezygotes and redistributed to the zygotic bud after fusion. This filipin staining pattern is consistent with a role for polarized ergosterol in pheromone signaling and plasma membrane fusion.

We next used *erg* mutant shmoos to examine the effect of sterol structure on filipin staining (Fig. 8 A). The percentage of shmoos with polarized filipin staining was strongly reduced in the *erg2*, *3*, and *6* mutants (Fig. 8 B), with a corresponding reduction in the ratio of shmoo tip to cell body filipin intensity. Filipin formed bright speckles on *erg6* cells that were randomly distributed over the surface of the cell and its mating projection. A lesser degree of speckling was found in the *erg2*, *3*, and *5* mutants (unpublished data). Speckling might result from filipin-induced sterol redistribution in strains with ergosterol precursors that can diffuse more rapidly in the plasma membrane (Valdez-Taubas and Pelham, 2003). In summary, the absence of a concentration of smoothly polarized filipin staining in mating projections correlates with defective pheromone signaling and plasma membrane fusion.

Surprisingly, filipin does not stain lipid rafts as was previously assumed. Mitotic cells stained poorly with filipin (Fig. 8 A), despite the fact that ergosterol represents 40% of plasma membrane lipids (Zinser et al., 1991; Schneiter et al., 1999). A potential explanation for this phenomenon is that ergosterol binds avidly to sphingolipids (Xu et al., 2001), which are also enriched in the plasma membrane, and that sphingolipids impede the access of filipin to ergosterol. This model was tested in *lcb1^{ts}* cells, which have a 50% reduction in sphingolipid synthesis when grown under permissive conditions (Zanolari et al., 2000; Hearn et al., 2003) and also have a modest reduction in the concentration of plasma membrane ergosterol (Baumann et al., 2005). Mitotic *lcb1^{ts}* cells had bright uniform filipin staining on their plasma membranes (Fig. 8 A). Equally bright filipin staining was found after treating *lcb1^{ts}* cells with α-factor, but the filipin was modestly polarized toward the shmoo tip (shmoo tip to cell body fluorescence ratios: wild type, 2.5 ± 0.7 [n = 40]; *lcb1^{ts}*, 1.5 ± 0.5 [n = 41]).

We considered several alternative explanations for the bright filipin staining of mitotic *lcb1^{ts}* cells. One possibility is that a compromised cell wall allows enhanced access of filipin to the plasma membrane. However, disrupting the cell wall integrity MAPK cascade with an *mpk1* deletion (Levin, 2005) does not enhance filipin staining (Fig. S5 A, available at http://www.jcb.org/cgi/content/full/jcb.200705076/DC1). Another possibility

is that the bright filipin staining of *lcb1*^{ts} cells is a secondary consequence of defects in endocytosis and actin organization. These defects can be suppressed by overproducing the Pkh1 or Ypk1 kinases, which are activated by sphingoid base intermediates in the sphingolipid biosynthesis pathway (Sun et al., 2000; Friant et al., 2001; deHart et al., 2002; Liu et al., 2005). However, *PKH1* and *YPK1* overproduction in *lcb1*^{ts} cells had no effect on filipin staining (Fig. S5 B). These results suggest that bright filipin staining of the *lcb1*^{ts} plasma membrane is a direct consequence of alterations in the lipid composition of the membrane.

Various steps in the sphingolipid biosynthetic pathway (Dickson et al., 2006) were inhibited to identify structural features that enable sphingolipids to inhibit the binding of filipin to ergosterol. The first step, conjugation of palmitoyl-CoA to serine to form sphingoid bases, was inhibited by myriocin (ISP-1). Addition of the second acyl chain, a C-26 very long chain fatty acid, was inhibited by fumonisin BI. Cells treated with either inhibitor stained brightly with filipin, which is consistent with the possibility that filipin staining is competitively inhibited by hydrophobic interactions between ergosterol and the long flexible acyl chains of sphingolipids (Fig. S5 C). The myriocin result was expected because *LCB1* encodes a subunit of serine palmitoyltransferase, the enzyme inhibited by myriocin. The fumonisin result further confirms that bright filipin staining is not a secondary consequence of reduced sphingoid base signaling because sphingoid bases accumulate in fumonisin-treated cells (Wu et al., 1995). In contrast to inhibiting acylation, inhibiting conjugation of mannose and phosphatidylinositol to the hydrophilic headgroups of sphingolipids by deleting the *CSG2* and *IPT1* genes did not give rise to bright filipin staining (Fig. S5 D). We conclude that acylated sphingolipids inhibit the interaction between filipin and ergosterol. Thus, the bright filipin staining at the tips of mating projections indicates a polarized accumulation of accessible sterols.

Ergosterol promotes PI(4,5)P_2 polarity

Because Ste5 binds to PI(4,5)P_2 (Winters et al., 2005; Garrenton et al., 2006), we wondered if PI(4,5)P_2 might also have a polarized distribution in mating yeast. Compared with ergosterol and sphingolipids, PI(4,5)P_2 is a minor component of the plasma membrane. It is concentrated on the cytoplasmic leaflet of the plasma membrane by virtue of local synthesis by Mss4 and degradation during endocytosis by lipid phosphatases homologous to synaptojanin (Stefan et al., 2002). PI(4,5)P_2 has been reported to associate with lipid rafts, but this proposal is controversial. PI(4,5)P_2 from mammalian cells floats with detergent-resistant membranes (Pike and Casey, 1996). In contrast, PI(4,5)P_2 has a negligible association with cholesterol by FRET, although the FRET signal can be substantially enhanced by addition of as little as 0.01% Triton X-100 (van Rheenen et al., 2005). Although PI(4,5)P_2 does not possess the long flexible acyl chains required for hydrophobic interactions between sphingolipids and sterols, interactions between PI(4,5)P_2 and sterols can be promoted by lipid raft–associated acidic proteins (Epand et al., 2004). Intracellular PI(4,5)P_2 was detected with 2×PH$^{PLC\gamma}$-GFP, a fusion of GFP to two copies of the pleckstrin homology domain of phospholipase Cγ (Stefan et al., 2002). In pheromone-treated yeast, 2×PH$^{PLC\gamma}$-GFP fluorescence was modestly concentrated on the surface of mating projections (Fig. 9 A). This polarized PI(4,5)P_2 localization was not an illusion resulting from the shape of the plasma membrane within the optical section because Sso2-GFP was not polarized under identical conditions. Interestingly, the intensity of 2×PH$^{PLC\gamma}$-GFP fluorescence was somewhat reduced at the very tip of the mating projection, where GFP-Ste5 is found. PI(4,5)P_2 could be less concentrated at the tip of the mating projection if this site is a target for exocytosis of PI(4,5)P_2-depleted secretory vesicles or for endocytosis and its associated PI(4,5)P_2-directed lipid phosphatases. Alternatively, an appearance of PI(4,5)P_2 depletion could result from competition for PI(4,5)P_2 binding between GFP-Ste5 and 2×PH$^{PLC\gamma}$-GFP (Balla et al., 2000), with GFP-Ste5 winning the contest at the shmoo tip because its localization there is reinforced by interactions with other polarized proteins. With respect to the potential role of lipid rafts in PI(4,5)P_2 localization, the *erg6* mutant had a 25% decrease ($P < 0.01$) in the percentage of shmoos with polarized 2×PH$^{PLC\gamma}$-GFP (Fig. 9 B). We conclude that a reduction in PI(4,5)P_2 polarization may contribute to reduced GFP-Ste5 recruitment and pheromone signaling upon ergosterol depletion.

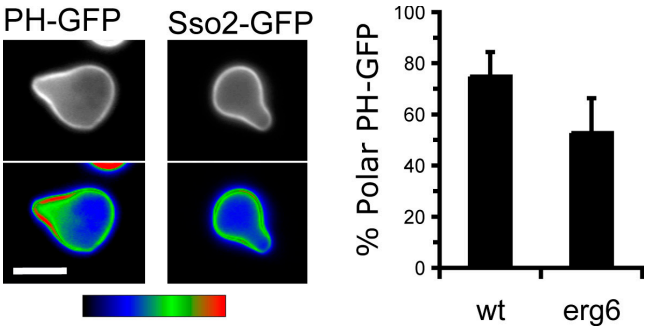

Figure 9. **Polarized PI(4,5)P_2 localization.** (A) α-factor–induced wild-type cells expressing 2×PH$^{PLC\gamma}$-GFP or Sso2-GFP. (B) Reduced PI(4,5)P_2 polarization in the *erg6* mutant. Bar, 5 µm. Error bars represent the standard deviation.

A balanced ergosterol to sphingolipid ratio promotes signaling

Signaling events at the cell surface are often confined within membrane microdomains enriched in both sterols and sphingolipids, which serve as platforms for protein complex assembly (Golub et al., 2004). In mammalian cells, these microdomains range in size from 10 to 200 nm and are therefore too small to be resolved by wide-field light microscopy (Jacobson et al., 2007). Thus, microdomains of sterol–sphingolipid interaction could be present at the tip of mating projections and at contact sites in prezygotes, despite our previous conclusion that these sites are enriched in sphingolipid-free ergosterol. As an alternative method to address the potential role of membrane microdomains in signaling, we measured pheromone responsiveness in *lcb1*^{ts} cells. Because the *lcb1*^{ts} mutation reduces the rate of sphingolipid synthesis (Zanolari et al., 2000; Hearn et al., 2003), *lcb1*^{ts} cells should have fewer ergosterol–sphingolipid complexes and an excess of free ergosterol. *FUS1* reporter expression was reduced by 70% in the *lcb1*^{ts} mutant, suggesting that the sphingolipid-associated pool of ergosterol is required for optimal signaling. More importantly, a 3-h FLZ pretreatment to deplete ergosterol enhanced

pheromone-induced P_{FUS1}-*lacZ* expression to near wild-type levels in the *lcb1*^{ts} mutant but had little effect on control cells (Fig. 10 A). These results were confirmed using myriocin as an alternative method to deplete sphingolipids at both 25 and 30°C (unpublished data). Thus, a balanced ergosterol to sphingolipid ratio is more critical for *FUS1* induction than the overall amount of either lipid. Quantitative measures of polarized morphogenesis in FLZ-treated cells support the P_{FUS1}-*lacZ* expression results. After a 3-h FLZ pretreatment, the percentage of cells that formed mating projections when challenged with 6 μM α-factor decreased by 40% in the wild type and increased by 20% in the *lcb1*^{ts} mutant, and the ratio of shmoo tip to cell body filipin fluorescence decreased by 30% in the wild type and increased by 20% in the *lcb1*^{ts} mutant. In conclusion, these results suggest that ergosterol and sphingolipids must assemble into stoichiometric complexes to promote pheromone signaling, which is consistent with the possibility that ergosterol/sphingolipid-enriched membrane microdomains serve as a platform to promote the association of Ste5 with Ste20 and other signaling proteins.

Sphingolipids have a minor role in plasma membrane fusion

Microdomains enriched in ergosterol and sphingolipids could potentially promote fusion by concentrating and activating fusion proteins. However, sphingolipid depletion with either the *lcb1*^{ts} mutation or the biosynthetic inhibitor myriocin did not interfere with plasma membrane fusion at normal total ergosterol levels. Thus, sphingolipids have a more critical role in pheromone signaling than in plasma membrane fusion. To further investigate the possible participation of membrane microdomains in fusion, wild-type and *lcb1*^{ts} cells were treated with FLZ before mating (Fig. 10 B). A 3-h FLZ pretreatment inhibited fusion to a similar extent in *lcb1*^{ts} mutant and control matings. However, after a 5-h FLZ pretreatment, the *lcb1*^{ts} mutant had a dramatically stronger fusion defect than the control. In summary, normal levels of total ergosterol promote efficient plasma membrane fusion even if sphingolipid synthesis is inhibited, but simultaneous depletion of ergosterol and sphingolipids revealed a secondary requirement for a low level of ergosterol–sphingolipid interaction. These results confirm that ergosterol has distinct functions in signaling and plasma membrane fusion.

Discussion

Ergosterol promotes at least two independent processes during mating. In response to mating pheromones, ergosterol promotes recruitment of Ste5 to the site of signaling on the plasma membrane. After mating pair assembly and cell wall remodeling, ergosterol facilitates plasma membrane fusion. Ergosterol is thought to interact with sphingolipids to promote the formation of membrane microdomains (lipid rafts) that concentrate the activity of associated membrane proteins. Pheromone signaling is highly sensitive to sphingolipid depletion, suggesting the involvement of lipid rafts, whereas sphingolipid depletion only interfered with plasma membrane fusion if ergosterol was also depleted. Thus, pheromone signaling and membrane fusion depend on different pools of ergosterol.

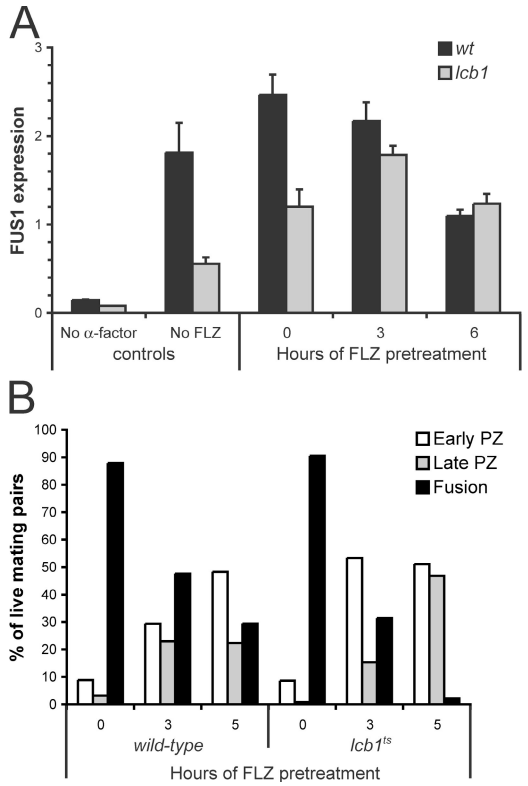

Figure 10. **Differential regulation of pheromone signaling and plasma membrane fusion by ergosterol and sphingolipids.** (A) Pheromone signaling. Error bars represent the standard deviation. (B) Plasma membrane fusion.

Ergosterol polarity in mating yeast

Ergosterol assumes a polarized distribution during mating. Filipin-accessible ergosterol is concentrated at the tips of mating projections and at sites of cell–cell contact in mating pairs. Although originally interpreted as a lipid raft marker (Bagnat and Simons, 2002), filipin actually stains sphingolipid-free ergosterol because staining is brighter in the *lcb1*^{ts} sphingolipid synthesis mutant. A recent study found that the general polarization of Laurdan fluorescence is strongest in mating projections (Proszynski et al., 2006). Laurdan provides an indication of lipid order by measuring water penetration into the lipid bilayer. In liposomes, lipid rafts have a high general polarization value, but it is not certain that this correlation extends to living cells. The filipin and Laurdan results clearly indicate that the tip of the mating projection has different lipid composition and packing than the cell body, but the exact nature of these differences requires further study. Nevertheless, the positive correlation among *erg* mutants between smoothly polarized filipin staining, strong pheromone signaling, and efficient plasma membrane fusion suggests that the local membrane environment must be properly controlled for efficient mating.

Sterols and sphingolipids promote pheromone signaling

Given that lipid rafts have long been considered as potential signaling platforms (Simons and Ikonen, 1997; Simons and Toomre, 2000), it is somewhat surprising that this study provides the first evidence that membrane lipids influence signal transduction in yeast. Pheromone-induced P_{FUS1}-*lacZ* transcription was attenuated

by the *erg2*, *3*, and *6* and *lcb1^{ts}* mutations and also by inhibiting ergosterol synthesis with FLZ or inhibiting sphingolipid synthesis with myriocin. The restoration of normal signaling when ergosterol and sphingolipids are both depleted provides compelling evidence that signaling depends on interactions between ergosterol and sphingolipids rather than on the function of either lipid in isolation. Two independent results indicate that ergosterol promotes plasma membrane–localized events in the signal transduction pathway. First, the *erg3* mutant had reduced recruitment of GFP-Ste5 to shmoo tips. Second, artificially targeting Ste5 to the plasma membrane partially suppressed the signaling defect resulting from FLZ pretreatment. These results do not exclude the possibility that ergosterol promotes membrane-associated signaling interactions before Ste5-GFP recruitment. The pheromone response pathway has multiple components whose interactions could be modulated by the local lipid environment (Fig. 5 A). These include seven transmembrane domain receptors (Ste2 and 3), lipid-anchored proteins (Ste18/Gγ and Cdc42), and proteins with lipid-binding motifs (Ste5 and Far1). In addition, interactions between $PI(4,5)P_2$ and ergosterol, as documented by reduced $PI(4,5)P_2$ polarization in the *erg6* mutant, may influence the localization and activity of $PI(4,5)P_2$ binding proteins such as Ste5 and Far1. Further investigation of the role of ergosterol, sphingolipids, and $PI(4,5)P_2$ in promoting interactions between signaling proteins should be conducted using methods, such as FRET, that can detect in vivo interactions on a submicroscopic scale (Jacobson et al., 2007).

Plasma membrane fusion in yeast mating pairs

The mechanism of plasma membrane fusion has been difficult to analyze because there are so few reagents that inhibit this step in the mating process. We have now identified three new mutations, *erg2*, *3*, and *6*, that cause an accumulation of mating pairs with plasma membranes that are in contact but not fused. This mating defect was documented by the presence of GFP- or RFP-labeled cytoplasmic fingers, which can only extend from a cell into its mating partner after the cell wall has been degraded, and by electron microscopy, where it is possible to directly observe an extensive zone of intimate contact between the two plasma membranes. The *erg* mutant phenotypes pointed to the involvement of ergosterol in plasma membrane fusion, and this was confirmed by the accumulation of late prezygotes after inhibiting ergosterol synthesis with FLZ or sequestering membrane ergosterol with nystatin. None of these mutations or treatments completely inhibits membrane fusion, possibly because ergosterol biosynthetic intermediates can partially replace the missing ergosterol. Two earlier studies reported mating defects for the *erg6* mutant but did not describe the critical contributions of ergosterol to signaling and membrane fusion (Tomeo et al., 1992; Bagnat and Simons, 2002).

The *prm1* and *erg6* mutations each inhibit plasma membrane fusion but they do so in different ways, as highlighted by the additive effect of deleting both genes. *prm1* mating pairs have a high propensity to lyse once the two membranes come into contact, whereas *erg6* mating pairs do not. We previously proposed that *prm1* lysis occurs via uncoordinated activation of the normal fusion machinery, but a definitive test of this model awaits the identification of a fusion protein (Jin et al., 2004). In our previous study, lysis was found to occur more frequently in time-lapse videos. The recent finding that extracellular Ca^{2+} increases the likelihood that *prm1* mating pairs will fuse rather than lyse (Aguilar et al., 2006) provides an explanation for this phenomenon. The optically clear agarose used for microscopy has a lower Ca^{2+} concentration than the crude agar used for plate mating assays. Ca^{2+} has been proposed to promote fusion by activating a membrane repair process that protects against lysis (Aguilar et al., 2006), but this model fails to explain why fusion of *prm1* mating pairs is also promoted by increasing membrane tension with a hypotonic shock (Nolan et al., 2006).

Recent reports have described two other mutations, *kex2* and *fig1*, that enhance the *prm1* fusion defect (Aguilar et al., 2006; Heiman et al., 2007). Kex2 is a Golgi-localized endoprotease involved in the processing of α-factor and a variety of other substrates. This protease activity is essential for the Kex2 plasma membrane fusion function but the relevant substrates are unknown. Arrested *kex2* mating pairs had membrane blebs and giant barren vacuoles that were not found in *erg6* or *prm1* mating pairs, suggesting that *kex2* defines a third independent function leading to membrane fusion (Heiman et al., 2007). Fig1 is a pheromone-inducible membrane protein that promotes Ca^{2+} influx during mating and is required for rapid cell death in response to high doses of α-factor (Erdman et al., 1998; Muller et al., 2003; Zhang et al., 2006). Because *fig1* mating pairs were originally found to arrest before cell wall remodeling (Erdman et al., 1998), we reexamined the *fig1* mating phenotype in both the BY4741 and W303 genetic backgrounds. After a 3-h mating, 3% of *fig1* mating pairs had arrested as late prezygotes. Thus, Fig1 appears to be a minor participant in the plasma membrane fusion process.

Sterols, sphingolipids, and membrane fusion

Sterols have many functions within membranes. In addition to their critical role in establishing membrane microdomains, they also modify membrane thickness, permeability, fluidity, and curvature. Which of these properties is relevant to plasma membrane fusion in mating yeast remains to be discovered, but the low sensitivity to sphingolipid depletion suggests that interactions between ergosterol and sphingolipids play a minor, although still potentially significant, role. Sterols are essential for many viral and intracellular membrane fusions (Salaun et al., 2004; Teissier and Pecheur, 2007). In contrast, immature sperm actually have higher cholesterol levels than the optimum for acrosome exocytosis (Belmonte et al., 2005). Sterol-dependent clustering of viral fusion proteins, cellular receptors, and SNAREs is critical for fusion in various systems, but these clusters can be distinct from biochemically defined lipid rafts (Lang et al., 2001; Percherancier et al., 2003; Takeda et al., 2003; Fratti et al., 2004; Yi et al., 2006). In addition, a protein clustering–independent role for cholesterol is supported by the partial restoration of fusion after adding lipids with negative curvature to cholesterol-depleted cortical granules (Churchward et al., 2005) and also by the observation that the optimal concentration of sterols and sphingolipids for protein-free liposome fusion matches the lipid composition of synaptic vesicles (Haque et al., 2001).

The data presented in this paper support a model whereby the sterol content of the plasma membrane determines its propensity to be fused by a Prm1-regulated protein complex. Inhibiting ergosterol synthesis increases the potential energy cost of fusion, but this barrier can be overcome by increasing the mating time or by amplifying the pheromone response. In the absence of Prm1, uncoordinated activity of the currently unknown fusion proteins is insufficient to fuse ergosterol-depleted membranes.

Materials and methods

Strains, reagents, and plasmids

The yeast strains used in this study were derived from strains produced by the *Saccharomyces* Genome Deletion Project (http://www-sequence.stanford.edu/group/yeast_deletion_project/deletions3.html) in BY4741 and BY4742 unless otherwise noted. Strains from the quality control collection of knockout strains were provided by M. Snyder (Yale University, New Haven, CT). The parental deletion strains were verified by PCR. *MATa* strains were transformed by the lithium acetate method with cytoplasmic GFP or plasma membrane–localized GFP-Sso2. *MATα* strains were transformed with either of two RFPs: DsRed or mCherry. The *prm1 erg* double-mutant strains were constructed by transformation of single mutants with a *prm1*::*HIS3* disruption plasmid. The *MATa ste5*^{ts} strain PPY423 (*MATa ste5-3*^{ts} *cry1 his4 leu2 lys2 tyr1 ura3 sup4-3*^{ts}) was obtained from P. Pryciak (University of Massachusetts Medical Center, Worcester, MA). A *MATα ste5*^{ts} strain was constructed by switching the mating type of PPY423 with a plasmid encoding the HO endonuclease. The *MATa lcb1*^{ts} *BAR1* strain EGMY600 was constructed by crossing RH2607 (*MATa lcb1-100 his4 ura3 leu2 bar1*; obtained from H. Reizman, Université de Genève, Geneva, Switzerland) to BY4742 *prm1* and backcrossing twice with BY4741. RH2607 (*lcb1*^{ts} *bar1*) failed to mate to an *erg6* partner, as previously shown (Bagnat and Simons, 2002). However, separating the *lcb1*^{ts} and *bar1* alleles revealed that *lcb1*^{ts} mates normally at 25°C, whereas mutations in the Bar1 α-factor protease cause a mating defect. The *mpk1* strain DL454 (*MATa mpk1::TRP1 leu2 trp1 ura3 his4 can1*^{R}, EG123) was obtained from D. Levin (Johns Hopkins Bloomberg School of Public Health, Baltimore, MD).

FM4-64 was purchased from Invitrogen. FLZ, nystatin, filipin, fumonisin BI, and myriocin were purchased from Sigma-Aldrich. α-Factor was synthesized by the Johns Hopkins Synthesis and Sequencing facility.

Plasmids are listed in Table I. pEG361 (*prm1::HIS3*) was constructed by inserting segments from the 5′ and 3′ UTRs of the *PRM1* gene into the XbaI and SphI sites of pRS303. The 5′ UTR segment from −526 to −207 was amplified with primers having 5′ SpeI and SphI extensions, and the 3′ UTR segment from 135 to 538 was amplified with primers having XbaI and SpeI extensions. pEG387 (*P*$_{TEF1}$*-GFP-PRM1*) was constructed by PCR amplifying the 2.3-kb coding sequence of *PRM1* with primers having 5′ EcoRI and SalI extensions, and then inserting the PCR product into pEG311 between the EcoRI and SalI sites at the 3′ end of the *GFP* coding sequence. pEG427 (*P*$_{GPD}$*-HA-PRM1*) was constructed by inserting PCR products encoding a 3×HA tag (Schneider et al., 1995) and a 5′ BamHI 3′ PstI-flanked *PRM1* open reading frame into p415GPD (Mumberg et al., 1995). The GPD promoter was then replaced by SacI–XbaI fragments containing the *CYC1*, *ADH1*, and *TEF1* promoters from p415CYC, p415ADH, and p415TEF (Mumberg et al., 1995) to construct pEG454, 455, and 456. pPP1551 was digested with SmiI to direct integration of *P*$_{FUS1}$*-GFP* to the 5′ UTR of *FUS1*. All PCR-generated plasmids were verified by DNA sequencing.

Light microscopy

Epifluorescent light microscopy was performed at room temperature with a motorized microscope (Axioplan 2; Carl Zeiss, Inc.) outfitted with a mercury arc lamp, band pass filters (Chroma Technology Corp.), differential interference contrast optics, and a digital camera (Orca ER; Hamamatsu). Single images were collected with a 100×/1.40 Plan Apochromat objective. Image fields were selected in an unbiased manner using differential interference contrast optics. Images were collected and their contrast was optimized with Openlab software (Improvision), using identical linear adjustments for all related images.

Time-lapse images of mating yeast were collected as previously described (Nolan et al., 2006). Mating mixtures were preincubated on filters over SC agar plates for 45 min. Cells were collected from the filters into 1 ml SC medium and concentrated to 20 µl by centrifugation. A 1.6-µl aliquot was then pipetted onto a 1.5-mm-thick pad of SC medium with 3% agarose on a microscope slide. Application of an 18-mm^2 coverslip caused the cell suspension to spread into an even layer. After excess agar was trimmed away, the slides were sealed with VALAP (a 1:1:1 mixture of petrolatum [Vaseline], lanolin, and paraffin) and observed during the period from 1 to 2 h after mixing. Time-lapse images were collected with

Table I. **Plasmids**

Name	Description	Source
pEG311	*P*$_{TEF1}$*-eGFP URA3 SSO1(CT)*	Jin et al. (2004)
pEG223	*P*$_{TEF1}$*-DsRed URA3 SSO1(CT)*	Jin et al. (2004)
pEG463	*P*$_{TEF1}$*-mCherry URA3 SSO1(CT)*	Nolan et al. (2006)
pEG361	*P*$_{TEF1}$*-eGFP-SSO2 URA3 SSO1(CT)*	Nolan et al. (2006)
pEG381	*prm1::HIS3*	This work
pEG387	*P*$_{TEF1}$*-eGFP-PRM1 URA3 SSO1(CT)*	This work
pEG427	*P*$_{GPD}$*-HA-PRM1 CEN LEU2*	This work
pEG454	*P*$_{CYC1}$*-HA-PRM1 CEN LEU2*	This work
pEG455	*P*$_{ADH1}$*-HA-PRM1 CEN LEU2*	This work
pEG456	*P*$_{TEF1}$*-HA-PRM1 CEN LEU2*	This work
pSM647	*P*$_{GAL1}$*-HO CEN URA3*	S. Michaelis[a]
pDL1399	*PKH1-HA 2µ URA3* (yEP352)	D. Levin
pDL267	*YPK1 2µ URA3* (yEP352)	D. Levin
pSB234	*P*$_{FUS1}$*-FUS1(1-254)-lacZ CEN URA3*	Trueheart et al. (1987)
pPP1551	*P*$_{FUS1}$*-GFP INT URA3*	P. Pryciak
pSKM21	*P*$_{CUP1}$*-STE5-GFP CEN URA3*	Mahanty et al. (1999)
pL38-WT	*P*$_{GAL1}$*-STE4 CEN HIS3*	Leberer et al. (1992)
pH-GS5-CTM	*P*$_{GAL1}$*-STE5-CTM CEN HIS3*	Pryciak and Huntress (1998)
pH-G11-Cpr	*P*$_{GAL1}$*-STE11-Cpr CEN HIS3*	Winters et al. (2005)
pGS11ΔN-L	*P*$_{GAL1}$*-GST-STE11ΔN CEN LEU2*	P. Pryciak
pNC252-HIS3	*P*$_{GAL1}$*-STE12 2µ HIS3*	P. Pryciak
pRS426GFP-2xPH(PLC)	*P*$_{CPY}$*-GFP-2xPH*$^{PLC\gamma}$ *2µ URA3*	Stefan et al. (2002)

[a]Johns Hopkins Medical Institute, Baltimore, MD.

a 63× Plan Apochromat objective lens. Both the objective lens and microscope stage were heated to 30°C, and binning (2×) was used to reduce exposure times and minimize photobleaching, with sets of GFP, DsRed, and differential interference contrast images collected sequentially at 15-s intervals.

Electron microscopy

Cells were fixed as previously described (Heiman and Walter, 2000) with minor modifications. In brief, cells were scraped off and fixed in 3% gluteraldehyde contained in 100 mM cacodylate, pH 7.4, with 5 mM Ca^{2+} for 60 min at room temperature. The cells were then washed twice with 100 mM cacodylate, once with water, and once with 3% $KMnO_4$ (Mallinckrodt). Cells were then fixed in 3% $KMnO_4$ for 60 min at room temperature, dehydrated through a graded series of ethanol (5′ washed with 50, 70, 80, 90, and 95% ethanol and 3 × 100% ethanol, 15 min each), and stored in a final wash of 100% ethanol overnight. Cells were then washed two times for 15 min each with propylene oxide (PO); placed into a 1:1 mixture of PO and Spurr resin; and subsequently placed under vacuum overnight. The next day, cells were transferred to 100% Spurr resin, left under vacuum for 24 h, and subsequently placed into beem capsules and allowed to polymerize at 60°C for 24–48 h. 80-nm sections were cut on an ultramicrotome (UCT; Leica), stained with lead citrate (Ted Pella, Inc.), and imaged with a transmission electron microscope (EM 410; Philips) equipped with a camera (Megaview III; Soft Imaging System). Figures were assembled in Photoshop (Adobe), with only linear adjustments in brightness and contrast.

Screening for cell fusion mutants

Strains from the quality control set of yeast deletion mutants were preferred for this screen because the *MATa* and *MATα* strains with a given mutation are arrayed in the identical position on two different sets of 96-well plates. Additional screening was performed on strains that were obtained from Invitrogen, which had to be rearrayed for bilateral mating tests. The strains were grown to saturation as a 96-well array in a 2-ml TiterBlock filled with a 3-mm glass bead and 1 ml of yeast peptone dextrose (YPD). Cells were then transferred to a fresh 96-well YPD TiterBlock using a pinning tool and grown in a shaker for 10 h at 30°C. Mating was initiated by pinning sequentially from the *MATa* and *MATα* TiterBlocks onto a nitrocellulose filter layered over a rectangular YPD plate. After incubating for 2.5 h at 30°C, the mating reaction was stopped by using a pinning tool to scrape the cells off the filter and then to mix them into 100 µl of ice-cold TAF buffer (20 mM Tris, pH 8.0, 20 mM NaN_3, and 20 mM NaF) in the wells of a round-bottom 96-well plate. Mating reactions could be stored for up to 2 d in TAF at 4°C before scoring. To score for mating defects, 2 ml of cells aspirated from the loose pellet at the bottom of each well were mixed into 2 µl FM4-64 (80 µM in H_2O on ice), and then loaded on a microscope slide. A coverslip was carefully layered over the FM4-64–stained cell suspension to wick the yeast into a monolayer without crushing the cells. The reaction was then visually scored for prezygote accumulation with reference to wild-type, *fus1*, and *prm1* standards (Fig. S1). No mutant that could form mating pairs had a complete block in cell fusion. Because several previously described cell fusion mutants had a low level of prezygote accumulation even in bilateral matings, the threshold for scoring prezygote accumulation was set at ∼5% of mating pairs. False positives were isolated at a frequency approaching 2% because of this low threshold. Isolated strains that grew to high density also contributed to the high rate of false positives. Many false positives were removed from the collection of putative mutants after repeating the primary screen with cells at closer to mid-log phase before the initiation of mating. For the secondary screen, the *MATa* strains of the putative cell fusion mutants were transformed with pEG311 for cytoplasmic GFP expression. *MATa* GFP strains were then mated to the corresponding *MATα* strains on 2.5-cm filters, following the standard mating assay procedure described in the following paragraph. When GFP transferred between two cells of a mating pair that appeared by FM4-64 staining to be arrested as a prezygote, we inferred that the fusion pore that allowed GFP transfer was either too small or too transient to be detected as a gap in the FM4-64–stained plasma membranes.

Mating assays

Mating assays were performed as previously described (Jin et al., 2004). 10^6 each of *MATa* and *α* cells growing in log phase were mixed and then collected on 2.5-cm-diam cellulose ester filters (Millipore). The filters were placed cell side up on SC agar plates and incubated for 100 min at 30°C unless otherwise indicated. Mated cells were collected from filters into ice-cold TAF buffer. The cells were concentrated by centrifugation for 5 s, resuspended in 20−30 µl TAF buffer, and analyzed by epifluorescent microscopy. At least 200 mating pairs were scored for all quantitative assays.

The standard mating conditions had to be adjusted to test for suppression of the *erg6* mating defect because Ste-CTM was expressed from a galactose-regulated promoter. Each pair of *erg6* strains was transformed with two plasmids containing different selectable markers: P_{GPD}*-PRM1 LEU2* or an empty vector control and P_{GAL1}*-STE5-CTM HIS3* or an empty vector control. The strains were grown to log phase in selective raffinose medium and then mated for 3 h at 30°C on galactose plates.

HA-Prm1 expression level comparisons

Yeast strains expressing the four *HA-PRM1* constructs were cultured to log phase in SC-leucine medium. Protein extracts were prepared by glass bead lysis from one OD_{600} unit of cells. Four 1:2 serial dilutions were prepared from each extract by dilution with an extract from an *sso1Δ* strain. Samples were resolved on a 10% SDS-PAGE gel, and a Western blot was cut into molecular weight-range strips that were separately probed with the 12CA5 anti-HA monoclonal antibody (Covance) and with an anti-Sso1 polyclonal antibody (Grote and Novick, 1999) as a loading control. The blot was developed by chemiluminescence with exposure times ranging from 5 s to 5 min. The films were digitized on a flatbed scanner, and band intensities were measured using Image software (National Institutes of Health).

GFP-Prm1 localization

MATa cells expressing *GFP-PRM1* from the *TEF1* promoter (pEG387) were mated for 1.5 h to *MATα fus1 fus2 RFP* cells to accumulate early prezygotes. To deplete ergosterol, the *MATa GFP-PRM1* cells were preincubated in YPD medium supplemented with 0.5 mg/ml FLZ for 3 h at 30°C and then mated to untreated *MATα fus1 fus2 RFP* cells on an SC + FLZ plate.

Pheromone response assays

Cells expressing P_{FUS1}*-FUS1(1–254)-lacZ* from pSB234 were grown to log phase in SC-uracil medium. The cells were pelleted and resuspended at OD_{600} 0.5 in medium supplemented with 6 µM α-factor and incubated for 90 min at 30°C unless otherwise indicated. For β-galactosidase assays, 0.4 OD_{600} units of cells were collected by centrifugation, resuspended in 100 µl Z buffer (82 mM $NaPO_4$, pH 7.0, 10 mM KCl, 1 mM $MgSO_4$, and 40 mM β-mercaptoethanol), and permeabilized by three rounds of freezing in liquid N_2 and thawing in a 37°C waterbath. Reactions were started by mixing 5–30 µl of the homogenate into 150 µl *o*-nitrophenyl-β-D-galacotpyranoside (1 mg/ml in Z buffer), incubated at 37°C for 10–90 min, stopped by the addition of 50 µl of 1 M Na_2CO_3, and read at OD_{410} in a 96-well plate reader (PerkinElmer).

To assay pheromone-induced GFP expression, P_{FUS1}*-GFP*–transformed cells were grown overnight in SC-uracil medium, treated in YPD medium with myriocin and/or FLZ as indicated, induced with 6 µm α-factor for 90 min at 30°C, and then washed with ice-cold TAF buffer. The GFP fluorescence of 20,000 cells was quantified in the FL1 channel of a FACSCalibur flow cytometer (BD Biosciences).

GFP-Ste5 localization

Cells transformed with pSKM21 were grown to log phase in SC-uracil medium. GFP-Ste5 expression was induced with 0.5 mM $CuSO_4$ for 2 h at 30°C. 2 × 10^6 cells were collected by centrifugation, resuspended in 400 µl SC-uracil/$CuSO_4$ + 6 µM α-factor, and incubated for an additional 30 min at 30°C. After α-factor treatment, the cells were again collected by centrifugation, resuspended in 10 µl SC-uracil/$CuSO_4$ + 30 µM α-factor, and immediately imaged. Live cells without buds were scored for GFP-Ste5 polarization. Varying degrees of polarization were observed, and strong polarization was found in only a small percentage of the cells. Thus, any cell with a detectable concentration of fluorescence associated with an arc spanning <45° on the cell surface was scored as positive for GFP-Ste5 polarization. The results are presented as mean ± 95% confidence intervals for four independent experiments, with $n > 150$ for each mutant in each experiment.

Filipin staining

The filipin staining procedure was based on a method developed for the study of *Schizosaccharomyces pombe* cytokinesis (Takeda and Chang, 2005). Filipin was added to live cells at a final concentration of 2.5 mg/ml in 0.5% DMSO. Cells were then concentrated by a brief centrifugation and imaged live within 1–5 min after filipin addition. The tips of *Saccharomyces cerevisiae* mating projections had somewhat brighter filipin staining than the growing end of mitotic *S. pombe* cells. Under these conditions, filipin did not compromise the viability of wild-type *S. cerevisiae*. This technique is therefore superior to previous methods for staining *S. cerevisiae* with filipin, which are prone to toxicity and artifacts (Valdez-Taubas and Pelham, 2003). Imaging filipin-stained cells was challenging because filipin is

rapidly bleached by UV excitation and its staining pattern became more speckled over time. To facilitate direct quantitative comparisons of filipin intensity and polarity, populations of wild-type and mutant cells marked by expression of either cytoplasmic GFP or Sso2-GFP were mixed before pheromone induction, staining, and imaging. For each mutant, at least 400 shmoos were scored blindly for filipin polarization and then categorized as wild-type or mutant.

$PI(4,5)P_2$ localization

Cells expressing $2\times PH^{PLC\gamma}$-GFP were induced with 6 μM α-factor for 90 min. For quantification, multiple fields of wild-type or *erg6* cells were scored blindly for mating projections with polarized fluorescence.

FLZ pretreatment

Cells in log-phase growth were pelleted, resuspended at low density (OD_{600} = 0.05) in appropriate growth medium, divided into 1-ml aliquots, and then grown in a shaking incubator at 30°C before α-factor treatment or at 25°C before mating (because *lcb1^{ts}* cells failed to form mating pairs at 30°C). 1 mg/ml FLZ was added to individual aliquots at the indicated times. Despite a significant amount of lysis leading to a slower apparent growth rate, the *lcb1^{ts}* mutation does not significantly alter the rate of ergosterol depletion in FLZ-treated cells. In a dose–response assay, 10 μg/ml FLZ was sufficient to maximally inhibit growth in both *LCB1* control and *lcb1^{ts}* mutant strains. In addition, FLZ treatment led to a 50–60% reduction in cellular ergosterol levels in both *lcb1^{ts}* mutant and control strains after 3 h at 30°C or 5 h at 25°C (Fig. S2).

Online supplemental material

Fig. S1 presents an overview of the genetic screening procedure that led to the identification of *erg6* and a plasma membrane fusion mutant and examples of mating pairs arrested at various stages of the cell fusion pathway. Fig. S2 presents critical controls related to the use of FLZ to deplete ergosterol, including growth curves and sterol analysis of wild-type and *lcb1^{ts}* mutant yeast. Fig. S3 presents results quantifying the relative activity in FLZ-treated cells of five plasmids that activate *FUS1* expression at distinct stages of the pheromone-response signal transduction pathway. Fig. S4 presents flow cytometry data for *ste5^{ts}* cells illustrating the gradual reduction in *FUS1* expression at elevated temperatures. Fig. S5 presents filipin-staining results demonstrating that bright filipin staining of sphingolipid-depleted plasma membranes is a direct consequence of alterations in the lipid composition of the membrane and that acylation, but not head-group, modification is required for sphingolipids to compete for ergosterol binding. Online supplemental material is available at http://www.jcb.org/cgi/content/full/jcb.200705076/DC1.

Thanks to John Burg and Peter Espenshade for sterol analysis and to Qing Huang for strain construction. Flow cytometry was performed in the laboratory of Dianne Griffin. Thanks to Peter Pryciak, Leonid Chernomordik, Elaine Elion, Charles Martin, Fred Chang, and members of the Grote Laboratory for advice and discussion, to Christopher Stefan for communicating results before publication, and to Peter Pryciak, David Levin, Michael Edidin, and Elizabeth Chen for comments on the manuscript.

This work was supported by a Research Scholar Award from the American Cancer Society.

Submitted: 14 May 2007
Accepted: 28 January 2008

References

Aguilar, P.S., A. Engel, and P. Walter. 2006. The plasma membrane proteins Prm1 and Fig1 ascertain fidelity of membrane fusion during yeast mating. *Mol. Biol. Cell.* 18:547–556.

Bagnat, M., and K. Simons. 2002. Cell surface polarization during yeast mating. *Proc. Natl. Acad. Sci. USA.* 99:14183–14188.

Balla, T., T. Bondeva, and P. Varnai. 2000. How accurately can we image inositol lipids in living cells? *Trends Pharmacol. Sci.* 21:238–241.

Bardwell, L. 2005. A walk-through of the yeast mating pheromone response pathway. *Peptides.* 26:339–350.

Baumann, N.A., D.P. Sullivan, H. Ohvo-Rekila, C. Simonot, A. Pottekat, Z. Klaassen, C.T. Beh, and A.K. Menon. 2005. Transport of newly synthesized sterol to the sterol-enriched plasma membrane occurs via nonvesicular equilibration. *Biochemistry.* 44:5816–5826.

Belmonte, S.A., C.I. Lopez, C.M. Roggero, G.A. De Blas, C.N. Tomes, and L.S. Mayorga. 2005. Cholesterol content regulates acrosomal exocytosis by enhancing Rab3A plasma membrane association. *Dev. Biol.* 285:393–408.

Brizzio, V., A.E. Gammie, G. Nijbroek, S. Michaelis, and M.D. Rose. 1996. Cell fusion during yeast mating requires high levels of a-factor mating pheromone. *J. Cell Biol.* 135:1727–1739.

Butty, A.C., P.M. Pryciak, L.S. Huang, I. Herskowitz, and M. Peter. 1998. The role of Far1p in linking the heterotrimeric G protein to polarity establishment proteins during yeast mating. *Science.* 282:1511–1516.

Chen, E.H., and E.N. Olson. 2005. Unveiling the mechanisms of cell-cell fusion. *Science.* 308:369–373.

Churchward, M.A., T. Rogasevskaia, J. Hofgen, J. Bau, and J.R. Coorssen. 2005. Cholesterol facilitates the native mechanism of Ca2+-triggered membrane fusion. *J. Cell Sci.* 118:4833–4848.

deHart, A.K., J.D. Schnell, D.A. Allen, and L. Hicke. 2002. The conserved Pkh–Ypk kinase cascade is required for endocytosis in yeast. *J. Cell Biol.* 156:241–248.

Dickson, R.C., C. Sumanasekera, and R.L. Lester. 2006. Functions and metabolism of sphingolipids in *Saccharomyces cerevisiae*. *Prog. Lipid Res.* 45:447–465.

Douglass, A.D., and R.D. Vale. 2005. Single-molecule microscopy reveals plasma membrane microdomains created by protein-protein networks that exclude or trap signaling molecules in T cells. *Cell.* 121:937–950.

Duelli, D., and Y. Lazebnik. 2003. Cell fusion: a hidden enemy? *Cancer Cell.* 3:445–448.

Elion, E.A. 2000. Pheromone response, mating and cell biology. *Curr. Opin. Microbiol.* 3:573–581.

Epand, R.M., P. Vuong, C.M. Yip, S. Maekawa, and R.F. Epand. 2004. Cholesterol-dependent partitioning of PtdIns(4,5)P2 into membrane domains by the N-terminal fragment of NAP-22 (neuronal axonal myristoylated membrane protein of 22 kDa). *Biochem. J.* 379:527–532.

Erdman, S., L. Lin, M. Malczynski, and M. Snyder. 1998. Pheromone-regulated genes required for yeast mating differentiation. *J. Cell Biol.* 140:461–483.

Fratti, R.A., Y. Jun, A.J. Merz, N. Margolis, and W. Wickner. 2004. Interdependent assembly of specific regulatory lipids and membrane fusion proteins into the vertex ring domain of docked vacuoles. *J. Cell Biol.* 167:1087–1098.

Friant, S., R. Lombardi, T. Schmelzle, M.N. Hall, and H. Riezman. 2001. Sphingoid base signaling via Pkh kinases is required for endocytosis in yeast. *EMBO J.* 20:6783–6792.

Gammie, A.E., V. Brizzio, and M.D. Rose. 1998. Distinct morphological phenotypes of cell fusion mutants. *Mol. Biol. Cell.* 9:1395–1410.

Garrenton, L.S., S.L. Young, and J. Thorner. 2006. Function of the MAPK scaffold protein, Ste5, requires a cryptic PH domain. *Genes Dev.* 20:1946–1958.

Golub, T., S. Wacha, and P. Caroni. 2004. Spatial and temporal control of signaling through lipid rafts. *Curr. Opin. Neurobiol.* 14:542–550.

Grote, E., and P.J. Novick. 1999. Promiscuity in Rab-SNARE interactions. *Mol. Biol. Cell.* 10:4149–4161.

Hancock, J.F. 2006. Lipid rafts: contentious only from simplistic standpoints. *Nat. Rev. Mol. Cell Biol.* 7:456–462.

Haque, M.E., T.J. McIntosh, and B.R. Lentz. 2001. Influence of lipid composition on physical properties and peg-mediated fusion of curved and uncurved model membrane vesicles: "nature's own" fusogenic lipid bilayer. *Biochemistry.* 40:4340–4348.

Hartwell, L.H. 1980. Mutants of *Saccharomyces cerevisiae* unresponsive to cell division control by polypeptide mating hormone. *J. Cell Biol.* 85:811–822.

Hearn, J.D., R.L. Lester, and R.C. Dickson. 2003. The uracil transporter Fur4p associates with lipid rafts. *J. Biol. Chem.* 278:3679–3686.

Heese-Peck, A., H. Pichler, B. Zanolari, R. Watanabe, G. Daum, and H. Riezman. 2002. Multiple functions of sterols in yeast endocytosis. *Mol. Biol. Cell.* 13:2664–2680.

Heiman, M.G., and P. Walter. 2000. Prm1p, a pheromone-regulated multispanning membrane protein, facilitates plasma membrane fusion during yeast mating. *J. Cell Biol.* 151:719–730.

Heiman, M.G., A. Engel, and P. Walter. 2007. The Golgi-resident protease Kex2 acts in conjunction with Prm1 to facilitate cell fusion during yeast mating. *J. Cell Biol.* 176:209–222.

Jacobson, K., O.G. Mouritsen, and R.G. Anderson. 2007. Lipid rafts: at a crossroad between cell biology and physics. *Nat. Cell Biol.* 9:7–14.

Jin, H., C. Carlile, S. Nolan, and E. Grote. 2004. Prm1 prevents contact-dependent lysis of yeast mating pairs. *Eukaryot. Cell.* 3:1664–1673.

Kato, M., and W. Wickner. 2001. Ergosterol is required for the Sec18/ATP-dependent priming step of homotypic vacuole fusion. *EMBO J.* 20:4035–4040.

Lang, T., D. Bruns, D. Wenzel, D. Riedel, P. Holroyd, C. Thiele, and R. Jahn. 2001. SNAREs are concentrated in cholesterol-dependent clusters that define docking and fusion sites for exocytosis. *EMBO J.* 20:2202–2213.

Leberer, E., D. Dignard, L. Hougan, D.Y. Thomas, and M. Whiteway. 1992. Dominant-negative mutants of a yeast G-protein beta subunit identify two functional regions involved in pheromone signalling. *EMBO J.* 11:4805–4813.

Levin, D.E. 2005. Cell wall integrity signaling in *Saccharomyces cerevisiae*. *Microbiol. Mol. Biol. Rev.* 69:262–291.

Lichtenberg, D., F.M. Goni, and H. Heerklotz. 2005. Detergent-resistant membranes should not be identified with membrane rafts. *Trends Biochem. Sci.* 30:430–436.

Liu, K., X. Zhang, R.L. Lester, and R.C. Dickson. 2005. The sphingoid long chain base phytosphingosine activates AGC-type protein kinases in *Saccharomyces cerevisiae* including Ypk1, Ypk2, and Sch9. *J. Biol. Chem.* 280:22679–22687.

Mahanty, S.K., Y. Wang, F.W. Farley, and E.A. Elion. 1999. Nuclear shuttling of yeast scaffold Ste5 is required for its recruitment to the plasma membrane and activation of the mating MAPK cascade. *Cell.* 98:501–512.

Mohler, W.A., G. Shemer, J.J. del Campo, C. Valansi, E. Opoku-Serebuoh, V. Scranton, N. Assaf, J.G. White, and B. Podbilewicz. 2002. The type I membrane protein EFF-1 is essential for developmental cell fusion. *Dev. Cell.* 2:355–362.

Mukherjee, S., and F.R. Maxfield. 2004. Membrane domains. *Annu. Rev. Cell Dev. Biol.* 20:839–866.

Muller, E.M., N.A. Mackin, S.E. Erdman, and K.W. Cunningham. 2003. Fig1p facilitates Ca2+ influx and cell fusion during mating of *Saccharomyces cerevisiae*. *J. Biol. Chem.* 278:38461–38469.

Mumberg, D., R. Muller, and M. Funk. 1995. Yeast vectors for the controlled expression of heterologous proteins in different genetic backgrounds. *Gene.* 156:119–122.

Munro, S. 2003. Lipid rafts: elusive or illusive? *Cell.* 115:377–388.

Nolan, S., A.E. Cowan, D.E. Koppel, H. Jin, and E. Grote. 2006. FUS1 regulates the opening and expansion of fusion pores between mating yeast. *Mol. Biol. Cell.* 17:2439–2450.

Ogle, B.M., M. Cascalho, and J.L. Platt. 2005. Biological implications of cell fusion. *Nat. Rev. Mol. Cell Biol.* 6:567–575.

Parks, L.W., and W.M. Casey. 1995. Physiological implications of sterol biosynthesis in yeast. *Annu. Rev. Microbiol.* 49:95–116.

Percherancier, Y., B. Lagane, T. Planchenault, I. Staropoli, R. Altmeyer, J.L. Virelizier, F. Arenzana-Seisdedos, D.C. Hoessli, and F. Bachelerie. 2003. HIV-1 entry into T-cells is not dependent on CD4 and CCR5 localization to sphingolipid-enriched, detergent-resistant, raft membrane domains. *J. Biol. Chem.* 278:3153–3161.

Pike, L.J., and L. Casey. 1996. Localization and turnover of phosphatidylinositol 4,5-bisphosphate in caveolin-enriched membrane domains. *J. Biol. Chem.* 271:26227–26232.

Podbilewicz, B., E. Leikina, A. Sapir, C. Valansi, M. Suissa, G. Shemer, and L.V. Chernomordik. 2006. The *C. elegans* developmental fusogen EFF-1 mediates homotypic fusion in heterologous cells and in vivo. *Dev. Cell.* 11:471–481.

Proszynski, T.J., R. Klemm, M. Bagnat, K. Gaus, and K. Simons. 2006. Plasma membrane polarization during mating in yeast cells. *J. Cell Biol.* 173:861–866.

Pryciak, P.M., and F.A. Huntress. 1998. Membrane recruitment of the kinase cascade scaffold protein Ste5 by the Gbetagamma complex underlies activation of the yeast pheromone response pathway. *Genes Dev.* 12:2684–2697.

Qi, M., and E.A. Elion. 2005. Formin-induced actin cables are required for polarized recruitment of the Ste5 scaffold and high level activation of MAPK Fus3. *J. Cell Sci.* 118:2837–2848.

Salaun, C., D.J. James, and L.H. Chamberlain. 2004. Lipid rafts and the regulation of exocytosis. *Traffic.* 5:255–264.

Schneider, B.L., W. Seufert, B. Steiner, Q.H. Yang, and A.B. Futcher. 1995. Use of polymerase chain reaction epitope tagging for protein tagging in *Saccharomyces cerevisiae*. *Yeast.* 11:1265–1274.

Schneiter, R., B. Brugger, R. Sandhoff, G. Zellnig, A. Leber, M. Lampl, K. Athenstaedt, C. Hrastnik, S. Eder, G. Daum, et al. 1999. Electrospray ionization tandem mass spectrometry (ESI-MS/MS) analysis of the lipid molecular species composition of yeast subcellular membranes reveals acyl chain-based sorting/remodeling of distinct molecular species en route to the plasma membrane. *J. Cell Biol.* 146:741–754.

Sharma, P., R. Varma, R.C. Sarasij, Ira, K. Gousset, G. Krishnamoorthy, M. Rao, and S. Mayor. 2004. Nanoscale organization of multiple GPI-anchored proteins in living cell membranes. *Cell.* 116:577–589.

Silva, L., A. Coutinho, A. Fedorov, and M. Prieto. 2006. Nystatin-induced lipid vesicles permeabilization is strongly dependent on sterol structure. *Biochim. Biophys. Acta.* 1758:452–459.

Simons, K., and E. Ikonen. 1997. Functional rafts in cell membranes. *Nature.* 387:569–572.

Simons, K., and D. Toomre. 2000. Lipid rafts and signal transduction. *Nat. Rev. Mol. Cell Biol.* 1:31–39.

Stefan, C.J., A. Audhya, and S.D. Emr. 2002. The yeast synaptojanin-like proteins control the cellular distribution of phosphatidylinositol (4,5)-bisphosphate. *Mol. Biol. Cell.* 13:542–557.

Sun, Y., R. Taniguchi, D. Tanoue, T. Yamaji, H. Takematsu, K. Mori, T. Fujita, T. Kawasaki, and Y. Kozutsumi. 2000. Sli2 (Ypk1), a homologue of mammalian protein kinase SGK, is a downstream kinase in the sphingolipid-mediated signaling pathway of yeast. *Mol. Cell. Biol.* 20:4411–4419.

Takeda, M., G.P. Leser, C.J. Russell, and R.A. Lamb. 2003. Influenza virus hemagglutinin concentrates in lipid raft microdomains for efficient viral fusion. *Proc. Natl. Acad. Sci. USA.* 100:14610–14617.

Takeda, T., and F. Chang. 2005. Role of fission yeast myosin I in organization of sterol-rich membrane domains. *Curr. Biol.* 15:1331–1336.

Teissier, E., and E.I. Pecheur. 2007. Lipids as modulators of membrane fusion mediated by viral fusion proteins. *Eur. Biophys. J.* 36:887–899.

Tomeo, M.E., G. Fenner, S.R. Tove, and L.W. Parks. 1992. Effect of sterol alterations on conjugation in *Saccharomyces cerevisiae*. *Yeast.* 8:1015–1024.

Trueheart, J., J.D. Boeke, and G.R. Fink. 1987. Two genes required for cell fusion during yeast conjugation: evidence for a pheromone-induced surface protein. *Mol. Cell. Biol.* 7:2316–2328.

Valdez-Taubas, J., and H.R. Pelham. 2003. Slow diffusion of proteins in the yeast plasma membrane allows polarity to be maintained by endocytic cycling. *Curr. Biol.* 13:1636–1640.

van Rheenen, J., E.M. Achame, H. Janssen, J. Calafat, and K. Jalink. 2005. PIP2 signaling in lipid domains: a critical re-evaluation. *EMBO J.* 24:1664–1673.

Viola, A., and N. Gupta. 2007. Tether and trap: regulation of membrane-raft dynamics by actin-binding proteins. *Nat. Rev. Immunol.* 7:889–896.

White, J.M., and M.D. Rose. 2001. Yeast mating: getting close to membrane merger. *Curr. Biol.* 11:R16–R20.

Whiteway, M.S., C. Wu, T. Leeuw, K. Clark, A. Fourest-Lieuvin, D.Y. Thomas, and E. Leberer. 1995. Association of the yeast pheromone response G protein beta gamma subunits with the MAP kinase scaffold Ste5p. *Science.* 269:1572–1575.

Winters, M.J., R.E. Lamson, H. Nakanishi, A.M. Neiman, and P.M. Pryciak. 2005. A membrane binding domain in the ste5 scaffold synergizes with gbetagamma binding to control localization and signaling in pheromone response. *Mol. Cell.* 20:21–32.

Wu, W.I., V.M. McDonough, J.T. Nickels Jr., J. Ko, A.S. Fischl, T.R. Vales, A.H. Merrill Jr., and G.M. Carman. 1995. Regulation of lipid biosynthesis in *Saccharomyces cerevisiae* by fumonisin B1. *J. Biol. Chem.* 270:13171–13178.

Xu, X., R. Bittman, G. Duportail, D. Heissler, C. Vilcheze, and E. London. 2001. Effect of the structure of natural sterols and sphingolipids on the formation of ordered sphingolipid/sterol domains (rafts). Comparison of cholesterol to plant, fungal, and disease-associated sterols and comparison of sphingomyelin, cerebrosides, and ceramide. *J. Biol. Chem.* 276:33540–33546.

Yi, L., J. Fang, N. Isik, J. Chim, and T. Jin. 2006. HIV gp120-induced interaction between CD4 and CCR5 requires cholesterol-rich microenvironments revealed by live cell fluorescence resonance energy transfer imaging. *J. Biol. Chem.* 281:35446–35453.

Zanolari, B., S. Friant, K. Funato, C. Sutterlin, B.J. Stevenson, and H. Riezman. 2000. Sphingoid base synthesis requirement for endocytosis in *Saccharomyces cerevisiae*. *EMBO J.* 19:2824–2833.

Zhang, N.N., D.D. Dudgeon, S. Paliwal, A. Levchenko, E. Grote, and K.W. Cunningham. 2006. Multiple signaling pathways regulate yeast cell death during the response to mating pheromones. *Mol. Biol. Cell.* 17:3409–3422.

Zinser, E., C.D. Sperka-Gottlieb, E.V. Fasch, S.D. Kohlwein, F. Paltauf, and G. Daum. 1991. Phospholipid synthesis and lipid composition of subcellular membranes in the unicellular eukaryote *Saccharomyces cerevisiae*. *J. Bacteriol.* 173:2026–2034.